PUBLICATIONS OF THE ASTRONOMICAL SOCIETY OF THE PACIFIC, **122**:1195–1206, 2010 October

A High-Contrast Imaging Survey of *SIM Lite* Planet Search Targets

ANGELLE M. TANNER,[1] CHRISTOPHER R. GELINO,[2] AND NICHOLAS M. LAW[3]

Received 2010 March 13; accepted 2010 July 28; published 2010 September 24

ABSTRACT. With the development of extreme high contrast ground-based adaptive optics instruments and space missions aimed at detecting and characterizing Jupiter- and terrestrial-mass planets, it is critical that each target star be thoroughly vetted to determine whether it is a viable target, given both the instrumental design and scientific goals of the program. With this in mind, we have conducted a high-contrast imaging survey of mature AFGKM stars with the PALAO/PHARO instrument on the Palomar 200 inch telescope. The survey reached sensitivities sufficient to detect brown dwarf companions at separations of >50 AU. The results of this survey will be utilized both by future direct imaging projects such as GPI, SPHERE, and P1640 and indirect detection missions such as *SIM Lite*. Out of 84 targets, all but one have no close-in (0.45–1″) companions and 64 (76%) have no stars at all within the 25″ field of view. The sensitivity contrasts in the K_s passband ranged from 4.5 to 10 for this set of observations. These stars were selected as the best nearby targets for habitable planet searches because of their long-lived habitable zones (>1 billion years). We report two stars, GJ 454 and GJ 1020, with previously unpublished proper motion companions. In both cases, the companions are stellar in nature and are most likely M dwarfs based on their absolute magnitudes and colors. Based on our mass sensitivities and level of completeness, we can place an upper limit of ~17% on the presence of brown dwarf companions with masses >40 M_J at separations of >1″. We also discuss the importance of including statistics on those stars with no detected companions in their field of view for the sake of future companion searches and an overall understanding of the population of low-mass objects around nearby stars.

1. INTRODUCTION

For the last decade, planet search efforts around nearby stars have been led by radial-velocity surveys that are sensitive to Jupiter-mass planets with close-in (<5 AU) orbits (Butler et al. 2006). High-contrast imaging surveys have recently culminated with the direct detection of Jupiter-mass planets at wider separations (>20 AU, Marois et al. 2008; Kalas et al. 2008). While the radial-velocity surveys are approaching sensitivities capable of detecting hot super-Earth mass planets around solar-mass stars and even habitable terrestrial-mass planets around some low-mass stars, Earth analogs remain out of reach, due to intrinsic stellar jitter. *Space Interferometry Mission Lite* (*SIM Lite*, formerly called *SIM PlanetQuest*, Unwin et al. 2008) will be the first instrument capable of detecting Earth analogs in the habitable zone of nearby stars. *SIM Lite* is a planned space-based interferometer with two 50 cm telescopes separated by 6 m. It is capable of achieving a single-measurement positional accuracy of 1 μas, enough to detect terrestrial planets in the habitable zone of nearby solar-type stars.

There are two *SIM* Key projects chosen to conduct surveys capable of detecting terrestrial-mass planets around nearby main-sequence stars—Discovery of Planetary Systems (Geoff Marcy, PI) and the Extrasolar Planets Interferometric Survey (EPIcS, Mike Shao, PI). These projects will carry out an astrometric search for rocky planets around ~200 stars located within 30 pc of the Sun.

There are many precursor programs currently being conducted to characterize and vet all potential targets for all the *SIM* Key projects (Unwin et al. 2008). These programs include radial-velocity studies of the reference stars utilized in the narrow-angle observations, accurate spectral type determinations through optical spectroscopy, and photometry studies of the stars in the young-star planet search program. Some of these programs have resulted in planet detections themselves (Niedzielski et al. 2007) or data that can be applied to upcoming planet surveys (Tanner et al. 2007). Here, we present the results of a companion survey of stars included in both of the terrestrial planet *SIM Lite* surveys. The observational goal of this companion survey is to identify bright nearby companions to the target stars. A companion with $\Delta V < 4$ and within 1″ can bias the position of the photocenter of the star, thus reducing the astrometric accuracy. While this survey was designed as a precursor program for *SIM Lite*, the observations presented here also serve as reconnaissance data for upcoming high-contrast imaging surveys such as the Gemini Planet Imager (GPI)

[1]Georgia State University, Department of Astronomy, One Park Place, Atlanta, GA; angelle.tanner@gmail.com.

[2]Infrared Processing and Analysis Center, 770 S. Wilson Ave. Pasadena, CA 91125.

[3]Dunlap Institute for Astronomy and Astrophysics, University of Toronto, 50 St. George Street, Toronto Ontario, Canada, M5S 3H4.

TABLE 1
PALOMAR AO SAMPLE

Target	R.A.	Decl.	μ_α (mas yr^{-1})	μ_δ (mas yr^{-1})	V	K_s	SpTy	Distance (pc)	Observing dates	$t_{\rm int}$ (s)
GJ 10	00 11 15.86	−15 28 04.72	−84	−269	4.89	3.82	F8V	18.89	2004 Aug; 2005 Nov	75; 400
GJ 15 A	00 18 22.89	+44 01 22.63	2889	410	8.07	4.02	M2V	3.57	2004 Oct; 2005 Nov	300; 500
GJ 15 B	00 18 25.87	+44 01 38.44	2912	351	11.04	5.95	M3.5	3.57	2004 Oct; 2005 Nov	1200; 500
GJ 1020	00 45 28.69	−12 52 50.92	−32	−206	6.15	4.62	G0V	31.86	2004 Dec; 2005 Nov	400; 200
GJ 34 B	00 49 05.17	+57 49 03.77	1105	−493	7.51	3.88	K7V	5.95	2004 Aug	105
GJ 34 A	00 49 06.29	+57 48 54.67	1087	−560	3.45	1.99	G0V	5.95	2004 Aug	150
GJ 37	00 50 07.59	−10 38 39.57	−225	−228	5.19	4.02	F7IV-V	15.46	2004 Dec 31; 2005 Nov	300; 400
GJ 61 A	01 36 47.84	+41 24 19.65	−173	−381	4.09	2.86	F8V	13.47	2004 Aug; 2005 Nov	45; 100
GJ 68	01 42 29.76	+20 16 06.62	−302	−677	5.20	3.29	K1V	7.47	2004 Aug; 2005 Dec	45; 350
GJ 71	01 44 04.08	−15 56 14.93	−1722	854	3.50	1.79	G8V	3.65	2004 Aug	4.5
GJ 72	01 44 55.82	+20 04 59.34	−45	−105	6.29	4.60	G5IV	32.56	2004 Aug; 2005 Dec	150; 140
GJ 79	01 52 49.17	−22 26 05.48	844	−1	8.88	5.18	K9Vk	11.09	2004 Aug	150
GJ 105 A	02 36 04.89	+06 53 12.73	1806	1442	5.82	3.48	K3V	7.21	2004 Aug	45
GJ 3175	02 40 12.42	−09 27 10.35	−138	−79	5.80	4.53	F6V	21.54	2004 Dec	790
GJ 107 B	02 44 10.26	+49 13 54.06	336	−84	9.87	5.87	M1.5	…	2004 Oct	1800
GJ 107 A	02 44 11.99	+49 13 42.41	334	−90	4.12	2.70	F7V	11.23	2004 Aug; 2004 Oct	100; 1800
GJ 111	02 45 06.19	−18 34 21.23	331	36	4.50	3.25	F6V	13.97	2004 Aug; 2004 Oct	40; 250
GJ 115 A	02 50 41.42	−44 04 52.69	−24	−272	8.19	6.70	F8V	58.28	2004 Aug	75
GJ 137	03 19 21.70	+03 22 12.71	269	94	4.83	2.96	G5Vv	9.16	2004 Aug	45
GJ 147	03 36 52.38	+00 24 05.98	−233	−482	4.28	2.84	F9IV-V	13.72	2004 Aug	63
GJ 204	05 28 26.10	−03 29 58.40	−307	−797	7.64	4.88	K5V	12.98	2004 Dec	2400
GJ 9207	06 16 26.62	+12 16 19.79	83	186	5.04	4.24	F5IV-V	19.61	2005 Nov	3000
GJ 250 B	06 52 18.07	−05 11 25.6	−541	0	10.05	5.72	M2	…	2005 Nov	600
GJ 302	08 18 23.95	−12 37 55.82	279	−989	5.95	4.17	K0V	12.58	2004 Dec	900
GJ 303	08 20 03.86	+27 13 03.75	−18	−376	5.10	3.87	F6V	18.13	2005 Nov	400
GJ 338 A	09 14 22.79	+52 41 11.85	−1533	−563	7.64	3.99	M0V	6.19	2004 Jun	5.4
GJ 338 B	09 14 24.70	+52 41 10.95	−1551	−656	7.74	4.14	M0V	6.27	2004 Jun	5.4
GJ 382	10 12 17.67	−03 44 44.38	−153	−243	9.26	5.02	M1.5	7.81	2004 Jun	300
GJ 394	10 30 25.31	+55 59 56.83	−181	−34	8.76	5.36	K7V	10.99	2004 Jun	50
GJ 423.1	11 18 22.01	−05 04 02.29	795	−151	7.31	5.46	G8V	21.99	2004 Jun	50
GJ 447	11 47 44.40	+00 48 16.43	606	−1219	11.08	5.65	M4	3.34	2004 Jun	110
GJ 448	11 49 03.58	+14 34 19.42	−499	−114	2.14	1.88	A3V	11.09	2004 Jun	360
GJ 454	12 00 44.45	−10 26 45.65	142	−483	5.54	4.03	K0IV	12.91	2004 Jun; 2005 Jul	3; 40
GJ 506	13 18 24.31	−18 18 40.31	−1070	−1064	4.74	2.96	G5V	8.53	2004 Jun; 2005 Jul	5.4; 60
GJ 526	13 45 43.78	+14 53 29.47	1778	−1455	8.46	4.41	M2V	5.43	2004 Jun	10
GJ 527 A	13 47 15.74	+17 27 24.86	−480	54	4.50	3.51	F6IV	15.60	2005 Jul	60
GJ 555	14 34 16.81	−12 31 10.40	−358	595	11.35	5.94	M4	6.12	2004 Jun	270
GJ 557	14 34 40.82	+29 44 42.47	188	133	4.46	3.34	F2V	15.47	2005 Jul	90
GJ 9491	14 43 03.62	−05 39 29.54	104	−320	3.90	3.04	F2V	18.68	2004 Aug	45
GJ 570 A	14 57 28.00	−21 24 55.71	1034	−1725	5.74	3.05	K4V	5.91	2004 Jun	480
GJ 581	15 19 26.83	−07 43 20.21	−1225	−100	10.57	…	M3	6.27	2004 Jun	480
GJ 598	15 46 26.61	+07 21 11.06	−226	−69	4.43	2.99	G0V	11.75	2004 Jun	600
GJ 602	15 52 40.54	+42 27 05.47	439	630	4.62	2.58	F8Ve...	15.85	2005 Jul	60
GJ 606.2	16 01 02.66	+33 18 12.63	−197	−773	5.40	3.86	G0Va	17.43	2005 Jul	90
GJ 616	16 15 37.27	−08 22 09.99	232	−496	5.50	4.19	G2Va	14.03	2004 Jun; 2004 Aug	960
GJ 628	16 30 18.06	−12 39 45.34	−94	−1185	10.12	…	M3.5	4.26	2004 Jun; 2004 Jul	10; 450
GJ 629.1	16 32 57.88	−12 35 30.23	−313	−226	10.61	7.25	M0	31.21	2004 Jun	450
GJ 663 A	17 15 20.85	−26 36 09.04	−488	−1156	5.29	…	K0V	5.46	2004 Jun	7.5
GJ 663 B	17 15 20.98	−26 36 10.18	−473	−1143	5.33	…	K1.5V	5.99	2004 Jun	7.5
GJ 664	17 16 13.36	−26 32 46.13	−480	−1123	6.34	…	K5V	5.97	2004 Jun	10
GJ 670 AB	17 21 00.37	−21 06 46.56	262	−205	4.39	3.07	F2V	17.40	2004 Jun	4
GJ 678 A	17 30 23.52	−01 03 54.6	−116	−170	6.00	…	G8IV-V	…	2004 Jun	90
GJ 687	17 36 25.90	+68 20 20.91	−320	−1270	9.15	4.55	M3.5V	4.53	2004 Jun; 2005 Nov	12; 150
GJ 692	17 43 25.79	−21 40 59.50	−98	−45	4.87	3.88	F5V	17.54	2004 Jun	5.4
GJ 699	17 57 48.50	+04 41 36.25	−799	10338	9.54	4.52	M4Ve	1.82	2004 Jun; 2005 Nov	12; 120
GJ 701	18 05 07.58	−03 01 52.75	570	−333	9.37	…	M1	7.80	2004 Jun; 2004 Aug	5.4
GJ 702 A	18 05 27.37	+02 29 59.32	276	−1092	4.20	1.79	K0V	5.09	2004 Jun; 2004 Aug	90

TABLE 1 (*Continued*)

Target	R.A.	Decl.	μ_α (mas yr^{-1})	μ_δ (mas yr^{-1})	V	K_s	SpTy	Distance (pc)	Observing dates	t_{int} (s)
GJ 702 B	18 05 27.42	+02 29 56.42	442	−1253	6.00	...	K4V	5.09	2004 Jun; 2004 Aug	6; 45
GJ 716	18 31 18.96	−18 54 31.72	−140	−195	6.82	4.70	K2V	13.21	2004 Jun; 2004 Aug	10
GJ 722	18 38 53.40	−21 03 06.74	−75	−152	5.87	4.23	G6V	12.98	2004 Jun; 2004 Aug	10
GJ 725 A	18 42 46.69	+59 37 49.43	−1327	1802	8.91	4.43	M3V	3.57	2004 Jun; 2004 Aug	12; 150
GJ 725 B	18 42 46.90	+59 37 36.65	−1393	1846	9.69	5.00	M3.5	3.52	2004 Jun; 2004 Aug	12; 150
GJ 726	18 47 27.25	−03 38 23.39	−133	−273	8.81	5.58	K5	14.12	2004 Jun	180
GJ 729	18 49 49.36	−23 50 10.44	638	−192	10.95	5.37	M3.5	2.97	2004 Jun; 2004 Aug	10
GJ 768	19 50 47.00	+08 52 05.96	537	386	0.77	0.10	A7V	5.14	2004 Jun	2
GJ 779	20 04 06.22	+17 04 12.62	−394	−406	5.80	4.39	G0V	17.67	2004 Jun; 2004 Aug	4; 42
GJ 785	20 15 17.39	−27 01 58.72	1241	−181	5.73	3.50	K2	8.82	2004 Jul	150
GJ 789	20 22 52.37	+14 33 03.95	79	−7	6.17	4.90	F8V	26.13	2004 Aug	100
GJ 796	20 40 11.76	−23 46 25.92	501	461	6.37	4.60	G8V	14.65	2004 Jun	130
GJ 805	20 46 05.73	−25 16 15.23	−51	−157	4.15	3.09	F5V	14.67	2004 Jul	150
GJ 811	20 56 47.33	−26 17 46.96	95	−65	5.70	4.48	F6V	21.00	2004 Jul	150
GJ 820 A	21 06 53.94	+38 44 57.90	4157	3259	5.21	2.25	K5V	3.48	2004 Jun; 2005 Nov	5.4
GJ 820 B	21 06 55.26	+38 44 31.40	4109	3144	6.03	2.54	K7V	3.50	2004 Jun; 2005 Nov	5.4
GJ 821	21 09 17.42	−13 18 09.02	710	−1995	10.87	...	M1	12.15	2004 Jun; 2005 Nov	270
GJ 848.4 A	22 09 29.87	−07 32 55.16	85	−450	6.63	4.89	G0V	21.29	2004 Jun	270
GJ 849	22 09 40.35	−04 38 26.62	1135	−20	10.42	5.59	M3.5	8.77	2004 Aug	500
GJ 872 A	22 46 41.58	+12 10 22.40	233	−492	4.20	2.96	F7V	16.25	2005 Jun	60
GJ 873	22 46 49.73	+44 20 02.37	−705	−459	10.09	5.30	M3.5	5.05	2004 Jun; 2005 Nov	10; 600
GJ 875	22 50 19.43	−07 05 24.39	−103	103	9.97	6.10	K7	14.00	2004 Oct	1800
GJ 876	22 53 16.73	−14 15 49.32	960	−676	10.17	...	M4	4.70	2004 Jul	650
GJ 882	22 57 27.98	+20 46 07.80	208	61	5.49	3.91	G5V	15.36	2005 Jun	180
GJ 884	23 00 16.12	−22 31 27.65	−904	58	7.89	4.48	K5V	8.14	2004 Jul	450
GJ 889 A	23 07 07.06	−23 09 34.01	154	−254	9.61	6.42	K6V	21.11	2004 Jul	650
GJ 892	23 13 16.98	+57 10 06.08	2075	295	5.56	3.26	K3V	6.53	2004 Jun	5.4
GJ 898	23 32 49.40	−16 50 44.31	344	−218	8.60	5.47	K6Vk	13.95	2004 Jul	900

(Macintosh et al. 2006), the VLT SPHERE coronagraph (Beuzit et al. 2008), and P1640, the recently commissioned Lyot adaptive optics (AO) coronagraph on the Palomar 200 inch (5 m) telescope (Hinkley et al. 2008). As a result of the high-contrast images collected for this survey, for most of the stars in the sample, we are sensitive to brown dwarf mass objects at separations of >50 AU. Because this program is sensitive to brown dwarf companions at wide separations, the results serve as an additional probe of the brown dwarf desert.

TABLE 2

TABLE OF OBSERVATIONS

Date	Seeing Conditions[a] ($''$)
2004 Jun 1–3	0.5
2004 Aug 1–3	1.0
2004 Oct 6–7	0.5
Nov 2004 11–14	0.7
2004 Dec 31	2.0
2005 Jul 7	1.5
2005 Nov 12–14	0.7
2005 Dec 7	3.0

[a] Seeing is estimated from the FWHM of one of the target stars observed with the adaptive optics turned off.

Section 2 describes the criteria by which we created the sample for the survey, § 3 details our observations, § 4 describes the data reduction and analysis, § 5 summarizes the results of the survey and our achieved sensitivities, and in § 6 we compare our results to previous surveys and discuss the importance of publishing nondetections.

2. SAMPLE SELECTION

The two *SIM Lite* terrestrial planet search programs coordinated their target selection so as to create unique lists for each team. Since one of the projects is primarily aimed at finding terrestrial planets in the habitable zone ("Extrasolar Planets Interferometric Survey [EPIcS]," Shao, PI) and the other is aimed at detecting all planets around stars within 8 pc ("Discovery of Planetary Systems," Marcy, PI), it was not difficult to agree on the two samples. Target stars were selected based on spectral type, heliocentric distance, brightness, companion separation (if applicable), habitable zone location, and the orbital period at the habitable zone.

Since these lists were created, the EPIcS program completed a study on how to further optimize the list. An additional sample

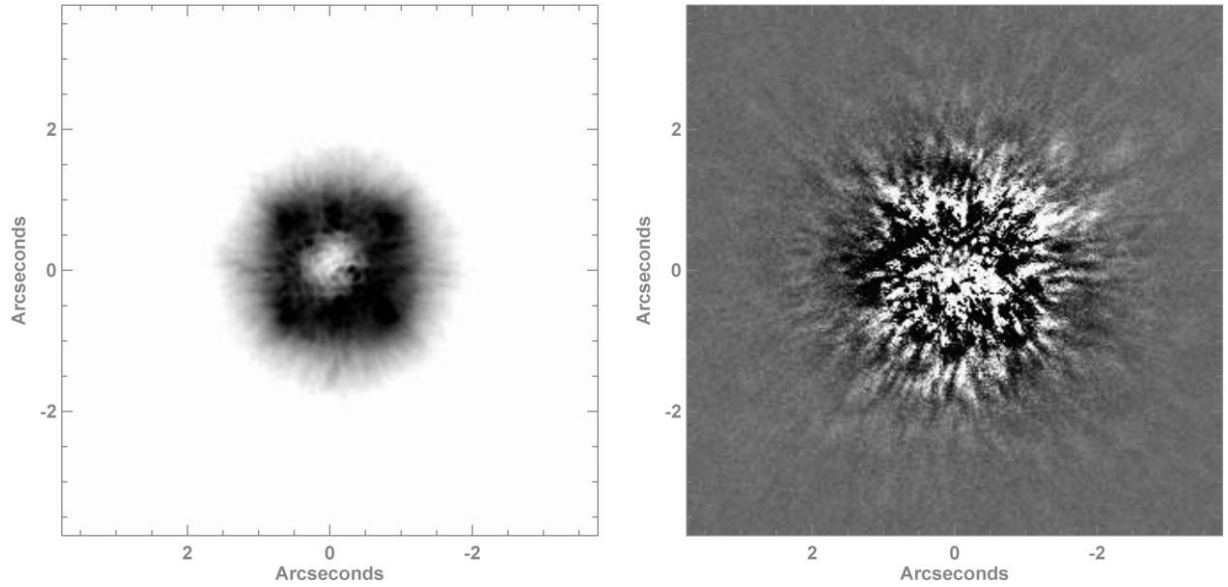

FIG. 1.—*Left*: Image of GL 876 prior to PSF subtraction. *Right*: The difference image between GL 876 and HD 216789 showing the reduced flux in the halo of the PSF as a result of the subtraction. North is up and east is to the left in all the images.

list of 240 stars has been created for the purpose of performing Monte Carlo simulations to predict the potential yield of a *SIM Lite* terrestrial planet search program (Catanzarite et al. 2006). This *SIM*-optimized target list is derived from an initial list of 2350 stars taken from the *Hipparcos* catalog, with distances of less than 30 pc (Turnbull & Tarter 2003). They excluded stars with luminosity greater than 25 times solar, thereby eliminating giants from our sample. To eliminate the possibility of fringe contamination from a binary companion, we applied the following: stars with a known companion closer than 0.4″ and $\Delta V < 4$ were excluded. If the target-star candidate had a wide binary companion that was separated by more than 1.5″, the companion was added to the list of target-star candidates. Further improvements on the target ranking will include considerations of stellar metallicity and the number and orientation of the reference stars with respect to the target. In the end, these stars will represent the best targets for a microarcsecond astrometric planet search.

After two years of observations, we have collected observations for a subset of 84 nearby main-sequence (V) stars taken from both the original EPIcS sample and the one created for Catanzarite et al. (2006). The properties of each of the stars in the sample are given in Table 1. The stars in our sample have distances of 3.5–30 pc, spectral types of M4-A3V, and V magnitudes of 0.77–11.35. Most, if not all, of the stars in the sample are mature stars with ages of 1–10 Gyr. We made sure not to reobserve those stars with published AO coronagraphic or *Hubble Space Telescope* observations (Carson et al. 2006; Lowrance et al. 2005; Metchev et al. 2005).

3. OBSERVATIONS

Observations were obtained with the Palomar Observatory Hale 5 m Telescope using the Palomar High Angular Resolution Observer (PHARO) near-IR camera (Hayward et al. 2001) behind the Palomar adaptive optics (PALAO) system (Troy et al. 2000). Observing dates and sky conditions are given in Table 2. We used a 25 mas pixel^{-1} scale camera (25″ field of view) and the 0.45″ radius occulting spot. Each star was observed in the K_s filter (2.16 μm) with integration times of 1–30 s, depending on the brightness of the star. Stacks of 20–100 short-exposure images were collected for each star, resulting in effective integration times of 100–1200 s.[4] Stacks of sky images were taken adjacent to each set of target images by offsetting 30″ from the target in the four cardinal directions and turning off the AO system. For flux calibration, observations of the target stars were taken by inserting the neutral-density filter, offsetting the star from the coronagraph and placing it in a five-point dither pattern to allow for adequate sky subtraction.[5] These offset images allowed us to determine that the FWHM of the AO-corrected observations varied from 0.2 to 1.3″ with Strehl ratios of 0.20–0.74. The seeing quality varies considerably for the

[4] Since the original *SIM Lite* Palomar survey started in 2004 was meant as a snapshot program intended to look for close stellar binaries, a subset of the coronagraphic observations was performed with a neutral-density filter that reduced the effective integration times by a factor of 100. In most cases, those stars were reobserved without the neutral-density filter to bring the effective integration times up to the level of the rest of the survey targets.

[5] Flux-calibration images were not collected during the 2004 June observing run.

TABLE 3
STARS WITH NO COMPANION CANDIDATES IN THE FIELD OF VIEW

GJ 10	GJ 628
GJ 34 A	GJ 629.1
GJ 34 B	GJ 663 A
GJ 37	GJ 663 B
GJ 61 A	GJ 664
GJ 68	GJ 670 B
GJ 71	GJ 678 A
GJ 79	GJ 687
GJ 107 A	GJ 692
GJ 111	GJ 699
GJ 137	GJ 702 B
GJ 147	GJ 725 A
GJ 167	GJ 725 B
GJ 204	GJ 768
GJ 303	GJ 785
GJ 338 A	GJ 796
GJ 382	GJ 805
GJ 394	GJ 811
GJ 423.1	GJ 820 A
GJ 447	GJ 821
GJ 448	GJ 849
GJ 506	GJ 872 A
GJ 526	GJ 875
GJ 527 A	GJ 876
GJ 555	GJ 882
GJ 557	GJ 884
GJ 570 A	GJ 889 A
GJ 581	GJ 898
GJ 598	GJ 3175
GJ 602	GJ 4324
GJ 606.2	GJ 9207
GJ 616	GJ 9491

different observing runs, from good (0.5″) to bad (>3″) based on the FWHM of the point-spread function (PSF) with no AO correction (see Table 2). The variable seeing affected our ability to achieve uniform sensitivities for all the target stars in the survey.

To aid in the suppression of speckle noise, we observed a set of PSF stars in conjunction with about half of our targets. The PSF stars were selected to have colors (i.e., spectral types), brightness, and air masses similar to those of the targets so as to produce a speckle pattern as close as possible to the science targets. Finally, sets of known binary stars with high-quality orbital solutions were also observed during the 2005 November and 2004 October runs to provide an accurate determination of the plate scale and image orientation. During the observation, each binary was placed in multiple positions over the field of view of the camera. In order to observe as many targets as possible while also reaching image sensitivities necessary to detect brown dwarf companions, our observing goal was to complete all observations associated with each target within a half-hour.

4. DATA REDUCTION AND ANALYSIS

The individual AO images were sky-subtracted, flat-fielded, and corrected for bad pixels, with the final image created from the median of the stack of reduced individual images. For those images with additional stars visible in the field of view, we used them to determine the offset of each image in the stack with respect to a reference image and shifted them accordingly prior to taking the median of the stack. This helped mitigate smearing from movement of the field during the observations due to telescope flexure or small losses in telescope tracking. A subset of the target images has corresponding observations of PSF stars with similar brightness and color. The relative positions of the target and PSF star were estimated using the Poisson spot present in the middle of the coronagraphic spot. As with previous studies (Metchev et al. 2004; Tanner et al. 2007), we are able to register the star positions to 0.7 pixels using the centroid position of the spot (Tanner et al. 2007). The scaling for the PSF is the multiplicative factor that minimizes the residuals remaining after the subtraction. Comparisons of the standard deviations of the speckle noise of the stars before and after PSF subtraction suggest that the subtraction reduced the noise within the halo by $\sim 25\%$. Figure 1 shows the difference image of GL 876 and its PSF star HD 216789.

The coronagraphic images were flux-calibrated using the images taken with the primary star offset from the coronagraph while accounting for a difference in integration time and the well-defined neutral-density filter used for the off-spot images (Metchev et al. 2004). The magnitudes for both the primary stars in the off-spot images and the companions in the coronagraphic images are estimated from aperture photometry with an aperture of 0.8″ and sky annulus of 1.–1.25″. The K_s-band magnitudes of the primaries were taken from the Two Micron All-Sky Survey (2MASS, Cutri et al. 2006). The uncertainties for the photometry were estimated from the errors given for the 2MASS magnitude and an assumption of a 5% calibration error determined by comparing the photometry of the companion to GJ 105a to published values (Golimowski et al. 2000).

The images of the calibration binaries were reduced in the standard manner. For the 2004 data, we assume a plate scale of 25.11 ± 0.04 mas pixel^{-1} estimated from the known orbital solutions of three different binary stars (WDS $09006+4147$, WDS $18055+0230$, and WDS $20467+1607$) that were observed very close to our October observations using the same instrument (2004 October 4–5, Metchev 2005, see their Table 4.1). For the 2005 data we estimate a plate scale of 25.21 ± 0.36 mas pixel^{-1} using the average and standard deviations of the measured pixel separation of one binary (WDS $09006+4147$, Hartkopf et al. 1996), compared to its predicted orbital separation in arcseconds. This binary, which was observed in 2005 November, was placed in multiple positions across the field of view after correction for the known distortion in the camera.

A thorough visual inspection of both the median-averaged coronagraphic images and the difference images between the

TABLE 4
COMPANION CANDIDATES

Target	$K_{starget}$[a]	Separation (″)	PA (°)	K_{scomp}	Epoch	Status[b]
GJ 15 A	4.02 ± 0.02	6.40 ± 0.12	158.3 ± 3.2	15.98 ± 0.06	2004 Oct	NCPM
GJ 15 B	5.95 ± 0.02	7.54 ± 0.12	66.2 ± 0.4	16.52 ± 0.06	2004 Oct	NCPM
		11.91 ± 0.14	70.3 ± 0.3	16.20 ± 0.06	2004 Oct	NCPM
GJ 72	4.60 ± 0.02	9.93 ± 0.12	−79.4 ± 0.4	11.85 ± 0.06	2004 Aug	NCPM
GJ 105 A	3.48 ± 0.21	2.63 ± 0.12	−54 ± 0.2	8.77 ± 0.22	2004 Aug	CPM[c]
GJ 107 B	5.87 ± 0.02	6.24 ± 0.12	161.3 ± 4.3	17.70 ± 0.06	2004 Oct	U
GJ 115 A	6.70 ± 0.02	6.50 ± 0.12	156.2 ± 2.5	18.81 ± 0.06	2004 Aug	U
GJ 250 B	5.72 ± 0.04	9.62 ± 0.13	−27.2 ± 1.4	14.04 ± 0.07	2005 Nov	U
GJ 302	4.17 ± 0.04	9.99 ± 0.13	−152.5 ± 1.3	15.46 ± 0.07	2004 Dec	NCPM
GJ 454	4.03 ± 0.26	0.99 ± 0.12	−75.5 ± 03.2	7.75 ± 0.06	2005 Jul	CPM
GJ 670 A	3.07 ± 0.30	10.79 ± 0.14	−98.9 ± 0.4	13.74 ± 0.38	2004 Jun	U
GJ 701	5.31 ± 0.02	12.36 ± 0.13	136.2 ± 0.3	…	2004 Aug	NCPM
GJ 702 AB	1.79 ± 0.30	9.38 ± 0.13	−128.9 ± 0.3	13.01 ± 0.30	2004 Aug	U
		11.53 ± 0.14	−164.5 ± 0.3	13.82 ± 0.30	2004 Aug	U
GJ 716	4.70 ± 0.02	2.84 ± 0.12	170.0 ± 3.2	14.06 ± 0.06	2004 Aug	NCPM
		3.54 ± 0.13	−92.8 ± 0.9	15.72 ± 0.06	2004 Aug	NCPM
		5.11 ± 0.13	−147.4 ± 1.4	15.75 ± 0.06	2004 Aug	NCPM
		5.30 ± 0.14	71.2 ± 1.2	15.91 ± 0.06	2004 Aug	NCPM
		5.38 ± 0.13	119.0 ± 1.6	13.62 ± 0.06	2004 Aug	NCPM
GJ 722[d]	4.23 ± 0.02	5.02 ± 0.12	−20.2 ± 5.4	15.90 ± 0.06	2004 Aug	NCPM
		6.40 ± 0.12	30.1 ± 1.5	17.50 ± 0.06	2004 Aug	NCPM
GJ 726[d]	5.58 ± 0.03	2.11 ± 0.12	−93.6 ± 1.5	13.63 ± 0.06	2004 Jun	U
		2.46 ± 0.12	−136.0 ± 1.4	14.31 ± 0.06	2004 Jun	U
		3.09 ± 0.12	−122.7 ± 1.0	17.62 ± 0.06	2004 Jun	U
		3.85 ± 0.12	−4.8 ± 1.2	16.42 ± 0.06	2004 Jun	U
GJ 729	5.37 ± 0.02	6.24 ± 0.12	−49 ± 0.5	17.04 ± 0.06	2004 Aug	U
		8.34 ± 0.13	−126.0 ± 0.4	17.70 ± 0.06	2004 Aug	NCPM
GJ 779	4.39 ± 0.03	3.30 ± 0.12	−77.5 ± 0.9	13.53 ± 0.06	2004 Aug	NCPM
		6.21 ± 0.12	162.0 ± 5.2	12.38 ± 0.06	2004 Aug	NCPM
		9.34 ± 0.13	140.1 ± 0.9	12.97 ± 0.06	2004 Aug	NCPM
GJ 789	4.90 ± 0.02	12.78 ± 0.14	67.9 ± 0.3	15.41 ± 0.06	2004 Aug	U
GJ 820 B	2.54 ± 0.33	11.51 ± 0.14	77.4 ± 0.4	14.8 ± 0.06	2005 Nov	U
GJ 848.4	4.60 ± 0.02	6.69 ± 0.12	−158.2 ± 3.1	16.5 ± 0.06	2004 Jun	U
GJ 873	5.30 ± 0.02	6.47 ± 0.12	175.5 ± 3.0	…	2005 Nov	U
		5.78 ± 0.12	115.6 ± 0.2	…	2005 Nov	U
GJ 892	3.26 ± 0.30	6.99 ± 0.12	44.5 ± 0.5	…	2004 Jun	NCPM
		9.93 ± 0.13	−17.9 ± 0.9	…	2004 Jun	U
		11.14 ± 0.12	−74.4 ± 0.8	…	2004 Jun	U
GJ 1020	4.62 ± 0.02	3.98 ± 0.12	−119.4 ± 0.7	10.34 ± 0.06	2004 Dec	CPM

[a] K_s magnitudes and errors taken from the 2MASS catalog (Cutri et al. 2006).
[b] NCPM is noncommon proper motion, CPM is common proper motion, and U is unconfirmed.
[c] Companion around GJ 105a was originally identified by Golimowski et al. 1995
[d] Star in crowded field. Not all companions in the field of view are listed.

targets and the PSF identified all stars in the 25″ field of view. Those target stars with no additional stars visible in the field of view are listed in Table 3, and the companion candidates identified in these images are listed in Table 4, along with their distance from the target star, position angle, and magnitude difference compared to the primary, when available. To accurately determine the position of the star behind the coronagraphic spot, we utilized the static waffle pattern, which has a distinct set of four speckles framing the PSF (see Fig. 2). As determined in Tanner et al. (2007), by using the centroid position of each of the four spots in the waffle pattern, we can use the intersection of the lines crisscrossing the pattern to determine the star's position to 2.3 pixels. This positional accuracy and the error in the plate scale are then propagated when determining the uncertainties for the offset and position angle.

4.1. Common Proper Motion Determination

For 13 of the stars with companion candidates, we collected second epoch observations at least a year later during AO

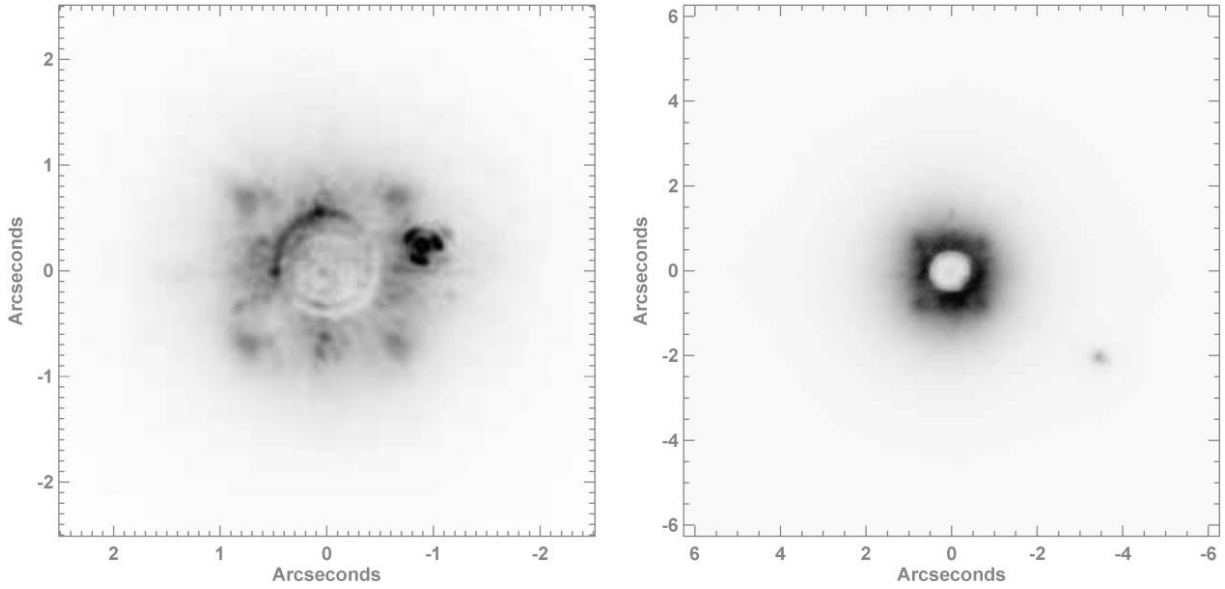

FIG. 2.—*Left*: Image of GL 454 and its common proper motion companion with a K_s magnitude of 7.75 and a separation of 0.95″. *Right*: Image of GL 1020 with a $K_s = 10.34$ magnitude companion 4″ away.

observing runs dedicated for other projects. The additional image allows us to determine whether the companion is bound to the star through their common proper motion. This positional accuracies given in Table 4 are sufficient to conclude whether the companion candidates are bound to their stars given the high proper motions (>100 mas yr^{-1}) of all the stars in the sample and the minimum of a full year between observations. In most cases, simply blinking between the images shows the movement of the background star once the target star is held fixed. We determined the separation and position angles of the candidates

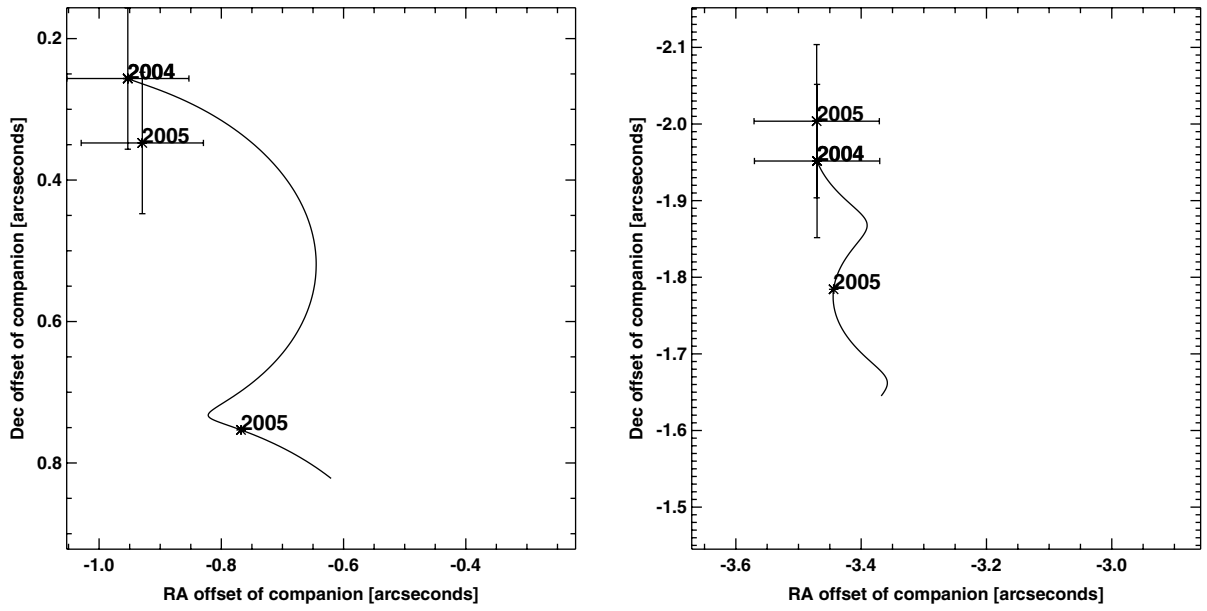

FIG. 3.—Plots of the offsets in right ascension and declination for the companion candidates around GL 454 and GL 1020. The squiggly line denotes the expected change in the offset if the companion were a background object. The labels (i.e., 2004, 2005) indicate the epochs of the observed offsets and the expected offsets of a background object at the epochs of the observations. The fact that the observed offsets are consistent with each other within the uncertainties suggests these two companions are bound to the star.

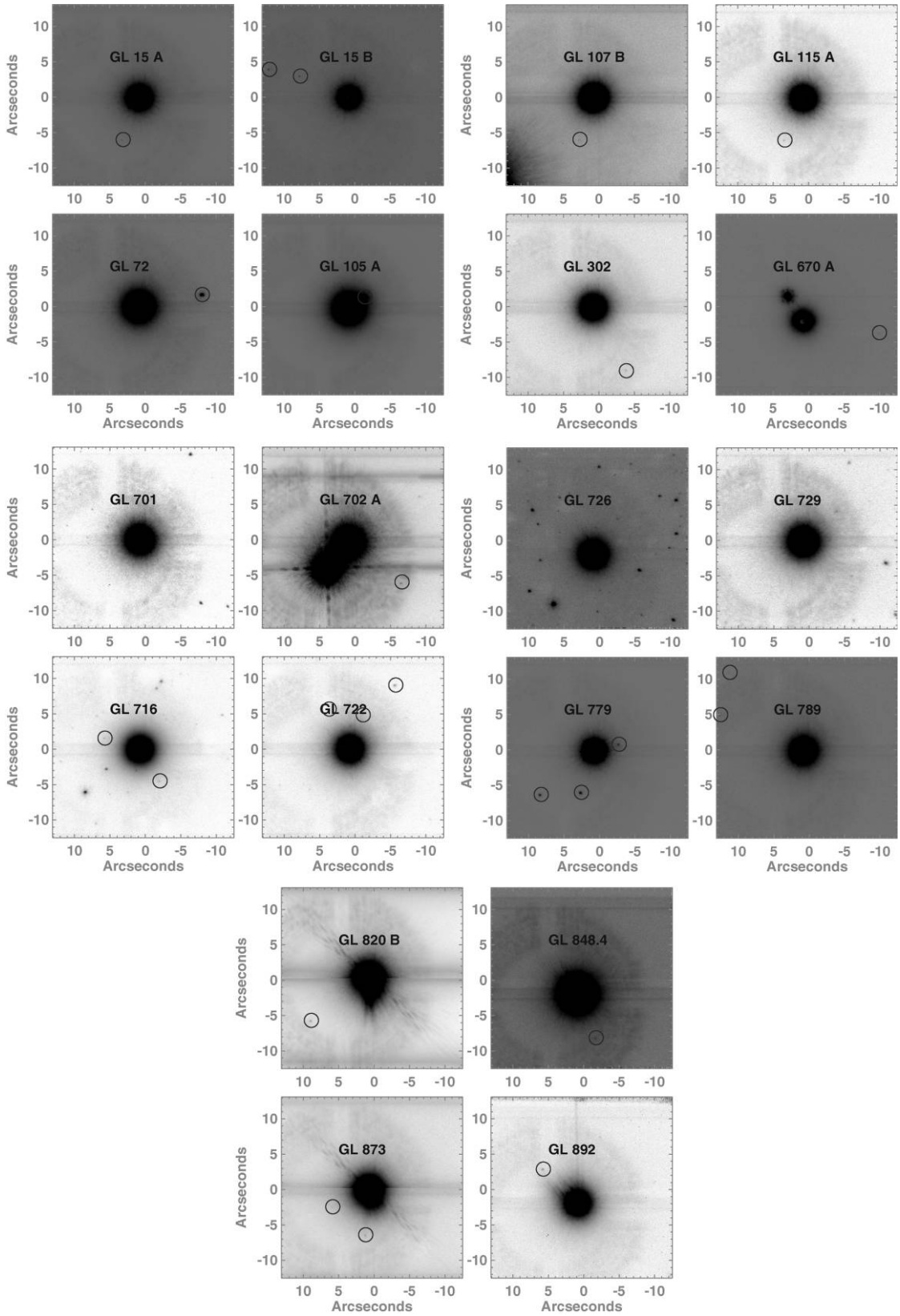

FIG. 4.—Images of the *SIM Lite* target stars with unidentified or confirmed background stars in their 25″ field of view. We have circled some of the stars to aid the reader.

TABLE 5
ASTROMETRY FOR CONFIRMED COMPANIONS

Target	ρ (")	PA (°)	Epoch
GL 454	0.987 ± 0.115	−75.06 ± 3.23	2004 Jun 4
	0.992 ± 0.115	−75.51 ± 3.12	2005 Jul 7
GL 1020	3.98 ± 0.12	−119.35 ± 0.74	2004 Dec 31
	4.01 ± 0.12	−119.97 ± 0.74	2005 Nov 14

in both images and compared them to what would be expected given the star's proper motion. After this analysis, we find two stars with confirmed common proper motion companions—GJ 454 and GJ 1020. The companions to these stars are new detections having not been mentioned in previous publications.

Figure 3 plots the offset in right ascension and declination between GL 454 and its companion 1″ away, and Table 5 lists the astrometry. The solid line denotes the expected motion of the companion if it were a stationary background object. The fact that the offset of the companion star estimated for two different epochs does not change significantly given the associated errors (10–30 mas) confirms this object as a bona fide companion. Additional observations of GJ 454 at 1.25 μm were made with the same instrument during the 2004 June run and were reduced in the same way as the K_s data. Given the K_s and J magnitudes of the companion ($K_s = 7.75$ and $J = 9.07$) and the distance to the star (12.91 pc), it is most likely an M3 dwarf (Baraffe & Chabrier 1996). Despite its proximity to GJ 454 and its relative brightness, $\Delta K_s > 6$, it should not pose a problem for *SIM Lite*. Figure 3 also shows the astrometry for the companion to GJ 1020, which was originally observed as a PSF star to GJ 10. This confirmed proper motion companion has a K_s magnitude of 10.4. With an absolute K magnitude of >10, this companion is most likely a low-mass star.

For some of the targets with no second epoch observations in our survey, we utilized images from the *HST*,[6] ESO,[7] and Gemini[8] archives. We were able to use these archive data sets to confirm that companion candidates around GJ 726, GJ 722, and GJ 892 are background stars. There are 17 companion candidates that remain unconfirmed (see Table 4 and Fig. 4).

5. RESULTS

Out of 84 stars, we found two unpublished common proper motion companions to GJ 454 and GJ 1020, neither of which will cause problems for *SIM Lite* observations, since it is much fainter than the target star. None of the companions have absolute magnitudes or colors consistent with brown dwarfs. This is not unexpected, given the observed paucity of brown dwarf companions to solar-mass main-sequence stars (McCarthy & Zuckerman 2004; Butler et al. 2006).

5.1. Image Sensitivities

To estimate the sensitivities of all of our target fields as a function of distance from the star, we employ "PSF planting," in which a PSF corresponding to an object of known brightness is inserted into the image. The PSF extracted from the off-spot

TABLE 6
PALOMAR IMAGING SENSITIVITIES, ΔK_s AT 90% COMPLETENESS

Target	0.5 (″)	1 (″)	2 (″)	5 (″)
GJ 10	6.32	6.54	7.91	10.20
GJ 1020	6.08	6.01	7.16	9.30
GJ 105a	5.82	5.93	7.25	9.29
GJ 107a	6.04	6.18	7.61	10.43
GJ 107b	7.52	8.33	10.21	12.77
GJ 111	6.31	6.44	8.02	9.74
GJ 115a	9.67	9.92	11.66	13.46
GJ 137	5.45	5.70	7.04	8.96
GJ 147	5.73	6.01	7.56	10.24
GJ 15a	6.61	6.95	7.99	10.24
GJ 15b	8.00	8.26	9.55	12.22
GJ 204	6.95	7.17	8.44	10.30
GJ 303	6.54	6.97	8.36	10.54
GJ 3175	6.86	6.98	8.48	10.20
GJ 37	6.16	6.25	8.06	9.95
GJ 454	5.56	5.79	7.35	8.45
GJ 506	5.24	5.36	6.23	8.54
GJ 527a	6.37	6.10	7.51	9.37
GJ 602	4.55	4.82	5.78	7.26
GJ 606.2	5.62	5.40	7.15	8.76
GJ 616	5.91	5.88	7.55	8.25
GJ 61a	7.60	8.25	9.75	12.21
GJ 629.1	9.56	8.64	10.02	10.93
GJ 68	6.04	6.33	7.83	9.79
GJ 699	6.19	6.54	8.60	11.08
GJ 702a	4.34	4.87	6.25	8.97
GJ 71	7.81	4.73	5.43	8.50
GJ 725b	6.57	6.94	8.08	9.72
GJ 729	7.51	7.72	8.79	9.97
GJ 779	6.98	6.97	8.81	10.38
GJ 785	5.98	6.19	7.64	10.29
GJ 789	7.31	7.57	6.84	9.18
GJ 805	5.70	5.72	6.84	9.18
GJ 811	6.62	6.61	7.51	9.25
GJ 820a	3.67	3.95	4.94	7.36
GJ 820b	4.44	4.54	5.75	7.78
GJ 849	7.84	8.11	9.70	12.00
GJ 872a	5.67	5.71	7.43	9.15
GJ 873	7.68	7.99	8.96	11.07
GJ 882	6.32	6.21	8.12	9.90
GJ 884	7.45	7.66	8.95	11.14
GJ 889a	8.18	7.92	9.05	9.45
GJ 898	9.54	9.91	10.00	12.35
GJ 9491	6.20	6.28	7.73	10.82

[6] See http://archive.stsci.edu/hst/.
[7] See http://archive.eso.org/cms/user-portal.
[8] See http://www1.cadc-ccda.hia-iha.nrc-cnrc.gc.ca/gsa/.

flux-calibration image of each target is sky-subtracted, normalized, multiplied by an array of contrast values ($\Delta K_s = 7.7$–15.1 mag), and placed at a range (0–10″) of distances from the target at random position angles. We completed 10^4 iterations of the PSF planting algorithm to fill out the parameter space of contrast and distance from the primary star. We make sure that the same number of planted PSFs occur in each radius bin. To determine whether the planted star is detected, the image is cross-correlated with a flux-normalized PSF. For each distance bin we estimate the minimum PSF intensity for which at least 90% of the fake sources had a correlation value of 0.75 or higher. This correlation value was determined by visually inspecting an image with inserted scaled PSFs. Previous studies have shown that the eye is often the best natural detector when determining the presence of a faint star in an image (Metchev et al. 2005).

The intensities are converted into magnitudes using the flux calibration from the off-spot image and the 2MASS K_s magnitude of the star. Figure 5 plots the largest K_s magnitude difference between the target star and planted PSF as a function of distance from the star for all targets with calibration data.

Table 6 lists the values of the faintest detectable K_s magnitudes at 0.5, 1, 2, and 5". We were able to detect sources with a magnitude contrast of $\Delta K_S \sim 4$–6.5 mag at 0.5″, $\Delta K_S \sim 5.5$–8 mag at 2″, and $\Delta K_S \sim 6.5$–9.5 at 5″ with ∼90% completeness. The range of image contrasts is due primarily to variations in seeing conditions throughout the night. Unfortunately, the brightest objects suffer from two additional components of degradation in image sensitivity: 1) a smudge in the optics that creates a long streak across the spot at a position angle of 45° and 2) a thick offset ring due to a reflection off the array, entrance windows, or the coronographic slide that is illuminating the Lyot stop (see Fig. 6). These image artifacts reduce the sensitivity in these areas of the image by 15–20%.

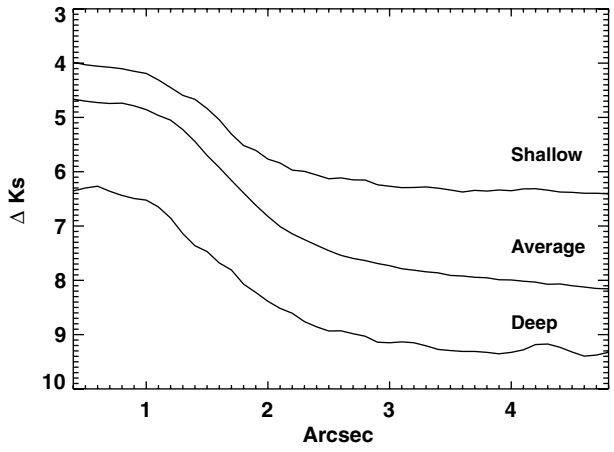

FIG. 5.—Plot of the differential magnitude detectable in the PHARO images as a function of distance from the star in arcseconds. The three lines represent the averages of three levels of sensitivity, which correspond to values at 3″ of $\Delta K_s > 6$, $5 < \Delta K_s < 4$, and $\Delta K_s < 4$ magnitudes, respectively. The sensitivity of any image depends both on the integration time of the exposure and the seeing conditions.

5.2. Mass Sensitivities

By assuming a set of values relating the absolute magnitude of any brown dwarf companion to its mass and age based on theoretical evolution models (Burrows et al. 1997; Baraffe et al. 2003), we can estimate an lower limit to the mass sensitivity around those target stars with flux calibrations. Figure 7 plots the lower limits of the mass sensitivity at a separation of 1″ from each star as a function of separation in AU based on its *Hipparcos* distance. The upper limits assume both 1 Gyr (crosses) and 5 Gyr (asterisks) ages for the primary star. This plot shows that most of our observations are reaching into the brown dwarf regime (∼75 M_J) at separations of 1″ and beyond.

6. DISCUSSION

6.1. How Does This Survey Compare with Previous Work?

There have been a few high-contrast surveys consisting of similar samples of nearby mature stars. Of those, the most notable include McCarthy & Zuckerman (2004), a large non-AO coronagraphic survey of a couple hundred nearby mature stars from which the brown dwarf desert was first posited at large (>100 AU) separations. Soon after this survey suggested that the percentage of mature stars with wide brown dwarf companions was comparable to the numbers determined from the radial-velocity surveys, ∼1%, additional coronagraphic AO

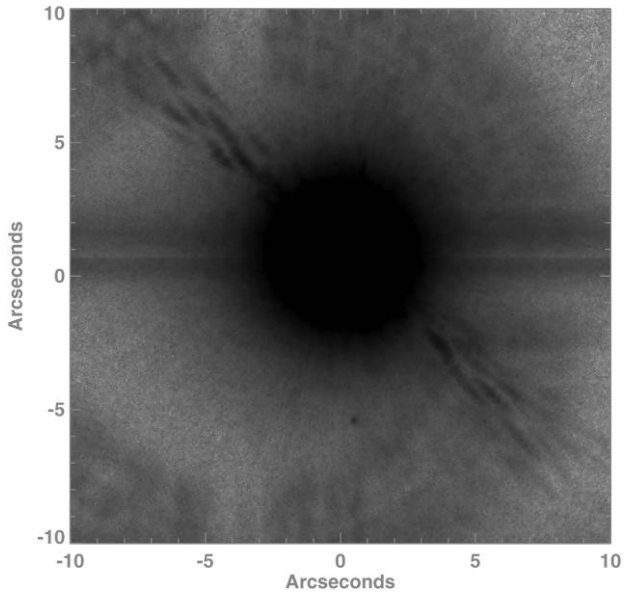

FIG. 6.—Image of GL 15 A using a histogram stretch to emphasize the scattered light from impurities in the optical path. These reflections, which are worse for bright stars, reduce contrast sensitivities by 15–20%.

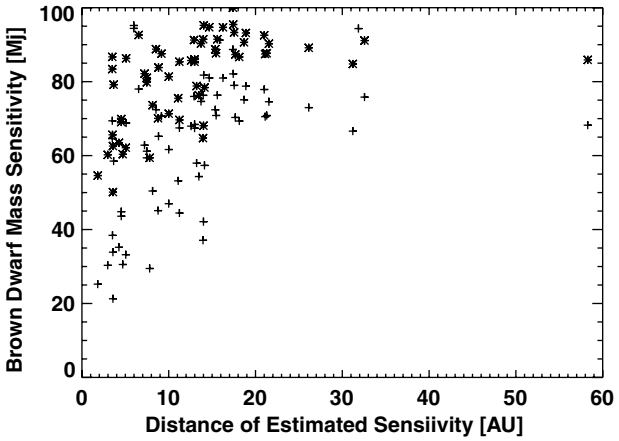

FIG. 7.—Minimum companion mass limits (Burrows et al. 1997) estimated from PSF planting as a function of projected physical distance from the star assuming ages of both 1 Gyr (crosses) and 5 Gyr (asterisks). We are sensitive to brown dwarf mass companions ($M < 75\ M_J$) for many of the stars in the survey.

surveys of similar targets suggested that this value is larger (3–10%), depending on the age of the targets and assuming noncircular orbits (Carson et al. 2005; Lowrance et al. 2005; Metchev et al. 2009). Based on our mass sensitivities and level of completeness, at a separation of 1" (>5–60 AU), we can place a 3σ upper limit of 17% on brown dwarf companions with masses down to $>40\ M_J$ at an age of 1 Gyr.

This survey presented here increases the sample of nearby mature (>1 Gyr) stars with high-contrast AO observations by over 50% when considering the "field" surveys listed in the table from Metchev et al. (2009). However, since the survey was originally designed as a precursor program to look for stellar companions to *SIM Lite* targets, our sample is not complete in a way that would allow us to provide improved limits on the brown dwarf companion fraction for the separations probed. However, these observations will be useful to future imaging surveys like GPI and SPHERE, which are expected to be sensitive to planetary-mass objects as well as brown dwarfs.

6.2. The Value of Publishing Nondetections

With projects like GPI, SPHERE, and *SIM Lite* being developed to focus almost primarily on the detection of exoplanets, it has become necessary to compile samples of targets that are going to yield the largest number of detections, given the strengths and weaknesses of the instruments. Therefore, many years before these projects see first light, much effort is devoted to target selection, verification, and precursor observations (i.e., Tanner et al. 2007; Carson et al. 2006). As a part of these precursor programs and as separate high-resolution studies focused on detecting brown dwarf and planetary-mass objects at wide separations, a large sample of stars have been observed with AO coronagraphic instruments. Unfortunately, in most cases, only those stars with companion candidates or confirmed companions are published. As a result, there are numerous unpublished observations of potential targets, resulting in repetitive observations of the same star in multiple studies. While these studies most likely have different inner working angles and overall sensitivities, there is value in having a public archive of previous observations to either weed out unknown close stellar binaries or to facilitate the identification of common proper motion. In fact, it was archival images of HR 8799 from a previously unpublished AO survey of nearby stars that was used to detect the orbital motion of the directly imaged planets in this system (Marois et al. 2008). In addition, the absence of companions up to a given mass at a given separation for a large sample of stars can provide just as much information on planetary formation and dynamics as their detection. With this in mind, all of the AO images collected for this survey will be donated to the NStED[9] database and we encourage others to do the same.

7. CONCLUSIONS

We have completed a high-contrast imaging survey of a sample of stars slated to be potential targets for the *SIM Lite* astrometric space telescope. While many of our observations were sensitive enough to detect brown dwarf companions at separations of $>1''$, our survey found two unpublished confirmed common proper motion stellar companions around GJ 454 and GJ 1020. This survey will serve as a resource for both *SIM Lite* and direct imaging surveys such as GPI and SPHERE, as all the images will be given to the NStED database. These images can be used to vet future targets and aid in common proper motion determinations. Additional *SIM Lite* targets will be observed with high-contrast imaging if they have not all ready been observed with other programs.

We would like to thank our anonymous referee for their valuable insights into how to improve our manuscript. We would also like to thank Shri Kulkarni and Mike Shao for invaluable discussions regarding the selection of the EPIcS targets. Based on observations obtained at the Hale Telescope, Palomar Observatory, as part of a continuing collaboration between the California Institute of Technology, NASA/JPL, and Cornell University. The research described in this publication was carried out at the Jet Propulsion Laboratory, California Institute of Technology, under a contract with the National Aeronautics and Space Administration. This publication makes use of data products from the Two Micron All Sky Survey, which is a joint project of the University of Massachusetts and the Infrared Processing and Analysis Center/California Institute of Technology, funded by the National Aeronautics and Space Administration and the National Science Foundation.

[9] See http://nsted.ipac.caltech.edu.

REFERENCES

Baraffe, I., & Chabrier, G. 1996, ApJ, 461, L51
Baraffe, I., Chabrier, G., Allard, F., Hauschildt, P. 2003, in IAU Symp. 211, Brown Dwarfs (San Francisco: ASP), 41
Beuzit, J.-L., et al. 2008, Proc. SPIE, 7014, 701418
Burrows, A., et al. 1997, ApJ, 491, 856
Butler, R. P., et al. 2006, ApJ, 646, 505
Carson, J. C., , Eikenberry, S. S., Brandl, B. R., Wilson, J. C., & Hayward, T. L. 2005, AJ, 130, 1212
Carson, J. C., Eikenberry, S. S., Smith, J. J., Cordes, J. M. 2006, AJ, 132, 1146
Catanzarite, J., Shao, M., Tanner, A., Unwin, S., & Yu, J. 2006, PASP, 118, 1319
Cutri, R., et al. 2006, AJ, 31, 1163
Golimowski, D. A., Fastie, W. G., Schroeder, D. J., & Uomoto, A. 1995, ApJ, 452, L125
Golimowski, D. A., Henry, T. J., Krist, J. E., Schroeder, D. J., Marcy, G. W., Fischer, D. A., & Butler, R. P. 2000, AJ, 120, 2082
Hartkopf, W. I., Mason, B. D., & McAlister, H. A. 1996, AJ, 111, 370
Hayward, T. L., Brandl, B., Pirger, B., Blacken, C., Gull, G. E., Schoenwald, J., & Houck, J. R. 2001, PASP, 113, 105
Hinkley, S., Oppenheiimer, B.-R., Brenner, D., Parry, I. R., Sivaramakrishnan, A., Soummer, R., & King, D. 2008, Proc. SPIE, 7015, 70519
Kalas, P., et al. 2008, Science, 322, 1345
Lowrance, P. J., et al. 2005, AJ, 130, 1845
Macintosh, B., et al. 2006, Proc. SPIE, 6272, L62720
Marois, C., Macintosh, B., Barman, T., Zuckerman, B., Song, I., Patience, J., Lafrenière, D., & Doyon, R. 2008, Science, 322, 1348
McCarthy, C., & Zuckerman, B. 2004, AJ, 127, 2871
Metchev, S. 2005, Ph.D. thesis, California Inst. of Technology
Metchev, S. A., & Hillenbrand, L. A. 2004, ApJ, 617, 1330
Metchev, S. A., & Hillenbrand, L. A. 2009, ApJS, 181, 62
Niedzielski, A., et al. 2007, ApJ, 669, 1354
Tanner, A., et al. 2007, PASP, 119, 747
Troy, M., et al. 2000, Proc. SPIE, 4007, 31
Turnbull, M. C., & Tarter, J. C. 2003, ApJS, 149, 423
Unwin, S. C., et al. 2008, PASP, 120, 38